Tunable Few-Cycle and Multicycle Coherent Terahertz Radiation from Relativistic Electrons

Yuzhen Shen, Xi Yang, G. L. Carr, Yoshiteru Hidaka, James B. Murphy, and Xijie Wang

Phys. Rev. Lett. **107**, 204801 — Published 11 November 2011

DOI: 10.1103/PhysRevLett.107.204801

Tunable Few-Cycle and Multi-Cycle Coherent Terahertz Radiation from Relativistic Electrons

Yuzhen Shen, Xi Yang, G. L. Carr, Yoshiteru Hidaka, James B. Murphy, and Xijie Wang

National Synchrotron Light Source, Brookhaven National Laboratory, Upton, NY 11973

Abstract

We report the generation of tunable, narrow-band, few-cycle and multi-cycle coherent terahertz (THz) pulses from a temporally modulated relativistic electron beam. We demonstrate that the frequency of the THz radiation and the number of the oscillation cycles of the THz electric field can be tuned by changing the modulation period of the electron beam through a temporally shaped photocathode drive laser. The central frequency of the THz spectrum is tunable from ~0.26 to 2.6 THz with a bandwidth of ~0.16 THz.

PACS number: 41.75.Ht, 42.72.Ai, 07.57.Hm

There is a growing interest in generating terahertz (THz) radiation for both scientific and technological applications. Intense single-cycle THz radiation from relativistic electrons has been demonstrated using linear accelerators.[1-3] The peak electric fields associated with these ultrashort electromagnetic pulses can exceed 10^7V/m, which offers the possibility to investigate novel ultrafast and nonlinear phenomena in the far-infrared frequency regime. A major obstacle to the wide application of accelerator-based THz sources is the lack of frequency tunability. This comes from the fact that the THz radiation is generated from a single electron bunch of ~1ps duration, which results in a single-cycle THz pulse with a broadband spectrum. Tunable THz radiation with a narrow spectral line width is of great interest for molecular spectroscopy, remote sensing, and imaging. A variety of techniques have been developed and applied to laser-based table-top THz sources to generate tunable THz radiation from photoconductive antennas and nonlinear media.[4-7] Recently, tunable THz radiation has also been produced from the laser-modulated electron bunches in a storage ring. An adjustable sinusoidal intensity modulation is applied to the laser that, in turn, interacts with relativistic electrons in a modulator to produce a corresponding density modulation on a submillimeter scale. Coherent THz radiation is then produced as synchrotron radiation from a dipole bending magnet.[8,9] To generate tunable THz pulses from linear electron accelerators, several approaches have been proposed but remained unexplored.[10-14] In this letter, we demonstrate for the first time that, by using a temporally shaped photocathode drive laser pulse, it is possible to control and manipulate the longitudinal charge distribution of a relativistic electron beam, and thereby generate tunable, narrow-band, few-cycle and multi-cycle coherent THz radiation. The result further widens the potential of existing accelerator facilities as sources of THz radiation.

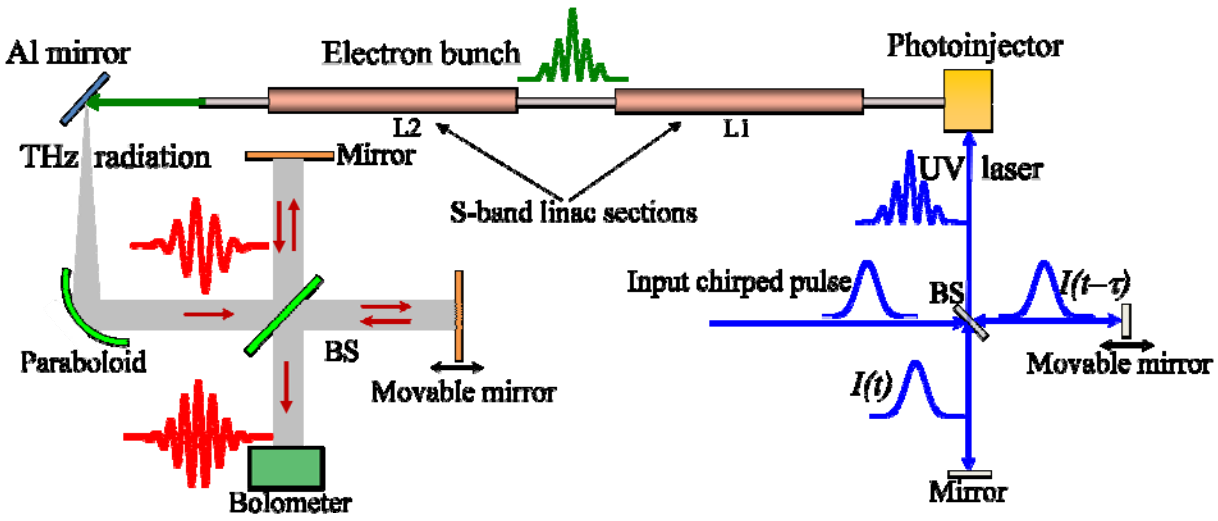

Figure 1. Schematic of a linac-based light source for tunable THz generation and characterization.

The THz source presented in this paper is developed at the Source Development Laboratory (SDL)[15] at Brookhaven National Laboratory, and a schematic diagram is shown in Figure 1. A magnesium photocathode in a radio-frequency photoinjector is illuminated by a frequency tripled Ti:sapphire laser amplifier at 265nm to produce photoelectrons with a 2.5Hz repetition rate. The ~100fs, 265nm pulse is temporally stretched and chirped using a pair of parallel diffraction gratings to ~6ps (FWHM), so that its instantaneous carrier frequency is linearly swept in time across the pulse duration. The chirped 265nm laser pulse is split into two pulses by a 50/50 beam splitter (BS), and one pulse is delayed by a variable interval τ with respect to the other. The two chirped pulses are then recombined. Consider a linearly chirped optical pulse with a Gaussian envelope and a quadratic temporal phase, which has an electric field,

, where E_0 is the amplitude, ω_0 is the carrier frequency,

¯ is the pulse duration, and b is the chirp rate. The superposition of this chirped pulse with its time-shifted replica leads to an output pulse [4]

(1)

The time difference between these two pulses produces a beat frequency, $\mu=2b\tau$, that is directly proportional to the time delay τ and the frequency chirp rate b. Therefore, the resultant output pulse has a Gaussian envelope modulated by a cosine function with a center frequency of $2b\tau$, which can be easily tuned by varying the time delay or the frequency chirp of the input pulses. Figure 2 shows the cross-correlation measurements of the temporal profiles of the photocathode drive laser pulses for different time delays. The modulation periods for Fig. 2(a) to 2(d) are ~5.0, 3.36, 1.38, and 0.6ps, corresponding to beat frequencies of 0.2, 0.31, 0.73, and 1.67THz.

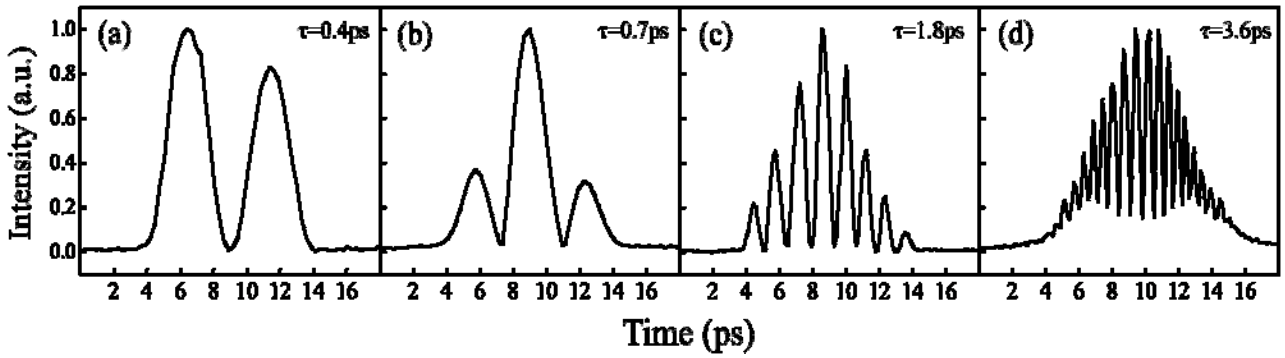

Figure 2. Temporal profiles of the photocathode drive laser pulses for different time delays.

Since the photoelectron emission from the cathode is prompt with respect to the laser light, the longitudinal distribution of the electron bunch is primarily determined by the temporal characteristics of the laser pulse. The electron bunch generated from the 5MeV photocathode has an energy chirp. The electrons at the bunch tail receive a higher energy gain and move faster than those at the head, leading to compression of the electron bunch.[16, 17] The electron bunch length and longitudinal profile are measured by the zero-phasing technique [18], in which a time correlated energy chirp is imposed on the bunch by passing it through an accelerator cavity on the zero crossing of the applied RF voltage (i.e. without net acceleration). The bunch is then dispersed by a dipole magnet, which is located after the last section of the linac, so that the different time slices of the electron bunch are projected onto a

scintillating screen at different horizontal positions, and thus the longitudinal profile of electron bunch is transformed into a transverse profile. The compression factor is measured to be ~1.3 for a ~100pC bunch. The electrons are then accelerated to the relativistic energy of ~120 MeV in two linac sections. The RF phase in the linac L1 is set to 15° off crest to remove the energy chirp, while the linac L2 is tuned for maximum acceleration. The electron beam longitudinal measurements are made for the different laser profiles shown in Figure 2. The top row of Figure 3 shows the corresponding longitudinal distribution for the temporally modulated electron bunches traveling down the linac. Projection of this distribution onto the longitudinal coordinate gives the electron density distribution, as shown in the bottom row of Figure 3. Due to the bunch compression, the modulation frequency of the electron bunch is ~1.3 times higher than that of the laser pulse. Space charge effects play a fundamental role in preservation of the temporal structure of the electron bunch. Although higher charge per bunch is desired for strong THz radiation; the charge that can be contained in a short bunch is limited by the space-charge force. At low charge, the space-charge effect is minimized by the rapid acceleration of the electron bunch to a relativistic energy, and the temporal structure of the electron bunch can be maintained through the acceleration. As shown in Figure 3, with ~100pC charge, the modulation frequency of the electron bunch can be as high as ~2.6THz, corresponding to a modulation period of ~ 385fs. As the bunch charge or the modulation frequency increases further, the density modulation is washout because the phase space of each electron bunch grows in both the longitudinal and energy coordinates, leading to the overlap of adjacent bunches.

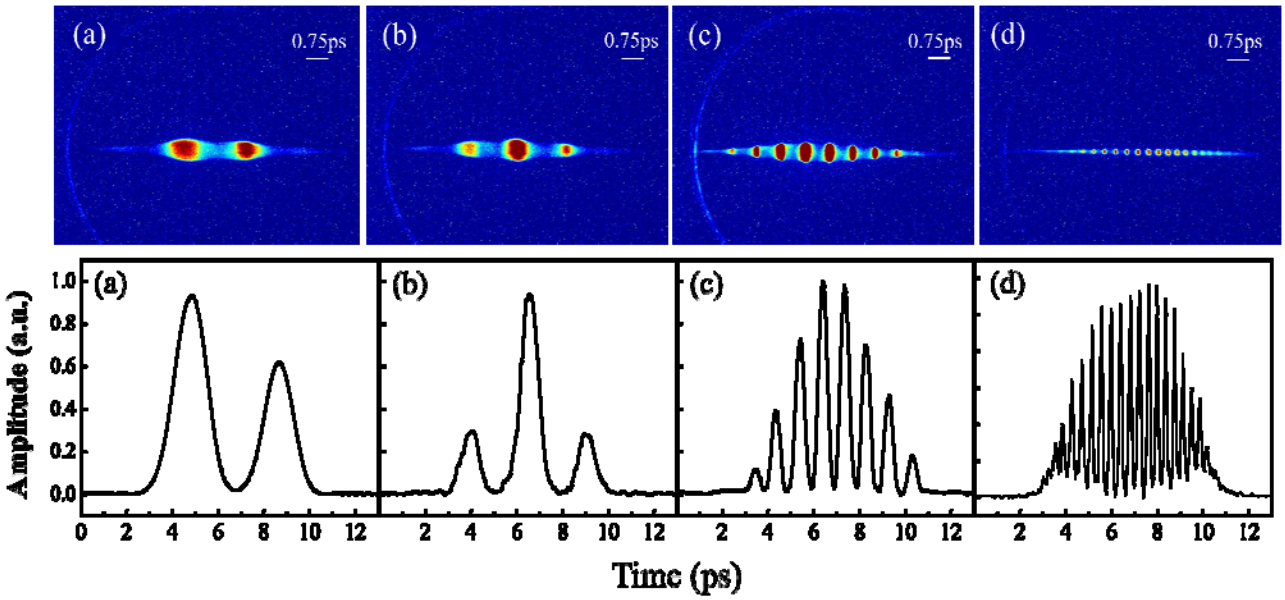

Figure 3. Measured longitudinal distribution (top row) and projected electron density distribution (bottom row) for a temporally modulated electron bunch.

As shown in Figure 1, after acceleration, the electron beam is incident onto a 2 cm diameter aluminum mirror oriented at 45° to the beam direction which generates transition radiation. The radiation spectrum is given by[19]

(2)

where is the energy spectrum generated by a single electron, is the number of electrons, and is the bunch form factor, which gives the radiation spectrum and is defined as the Fourier transform of the electron temporal distribution. For the moment, we will ignore the bunch compression effects. Since the electron temporal distribution follows the laser intensity modulation, it can be approximated by Equation 1. The first two terms in the equation corresponds to the slowly varying Gaussian envelope, which gives the DC spectral component centered at ω=0. The cross term, , contains the sinusoidal modulation. Its Fourier transform determines the bunch factor. Since only defines the initial phase for each delay, it can be neglected in this analysis. For a relativistic

bunch whose transverse dimensions are small compared to the bunch length the form factor becomes

$$f(\omega) = [\int S(t) \exp(i\omega t)\, dt]^2 = 4 \exp(-\alpha\tau^2) \exp\left(-\frac{(\omega-\mu)^2}{4\alpha}\right) \quad (3)$$

which indicates coherent radiation at the modulation frequency μ for each delay τ, and therefore the tunable coherent THz radiation can be obtained by using the photocathode drive laser to apply a quasi-sinusoidal modulation on the electron bunch at THz frequencies. From equations 2 and 3, the form factor and radiation energy will drop with increasing the time delay and the THz frequencies.

Since the accelerating charges induce a transient current and generate an electromagnetic field, the electric field is related to the transient current, i(t), by $\mathrm{E(t)} = \partial \mathrm{i(t)}/\partial \mathrm{t}$. For coherent radiation from a single electron bunch having a Gaussian longitudinal distribution, the induced transient current has a Gaussian time-dependence. The electric field of the THz radiation follows the temporal derivative of the current, leading to a single-cycle THz waveform, as has been demonstrated over the past few years.[1-3] However, by using a quasi-sinusoidal electron bunch, few-cycle or multi-cycle THz radiation can be synthesized while the THz frequency is tuned.

As shown in Figure 1, the coherent THz radiation is extracted from the accelerator vacuum pipe through a 2.5-inch diameter z-cut crystalline quartz window. The divergent THz radiation is collimated by a parabolic mirror into a parallel beam which enters a far-infrared Fourier transform spectrometer based on a step-scan Michelson interferometer with a 25μm Mylar beam splitter and a helium-cooled silicon composite bolometer as detector. The field autocorrelation of the THz radiation is recorded by varying the time delay of one arm of the interferometer with respect to the other. Figure 4 shows the THz interferograms obtained for different laser and

electron bunch profiles shown in Figure 2 and 3. With DC offset subtracted, the Fourier transform of the interferogram gives the power spectra of THz radiation, as shown in Figure 5. The THz radiation is narrow-band with central frequencies at ~ 0.26, 0.4, 1.1, and 2.6THz, consistent with the modulation frequency of the electron bunch. The spectral bandwidth for different central wavelengths is ~ 0.16THz, as expected for the known macropulse length. The interferogram exhibits an oscillation with a period of half the radiation wavelength, which provides a direct and accurate self-calibration of the measurement. A train of N electron bunches whose amplitude is quasi-sinusoidally modulated results in an interferogram with 2N-1 peaks and gives rise to N-cycles of the electromagnetic field. Figure 4(a) and 4(b) indicate the THz electric field consists of essentially 2 and 3 oscillation cycles. Figure 4(c) and 4(d) show the formation of multi-cycle THz radiation with increasing time delay τ between the two chirped laser pulses.

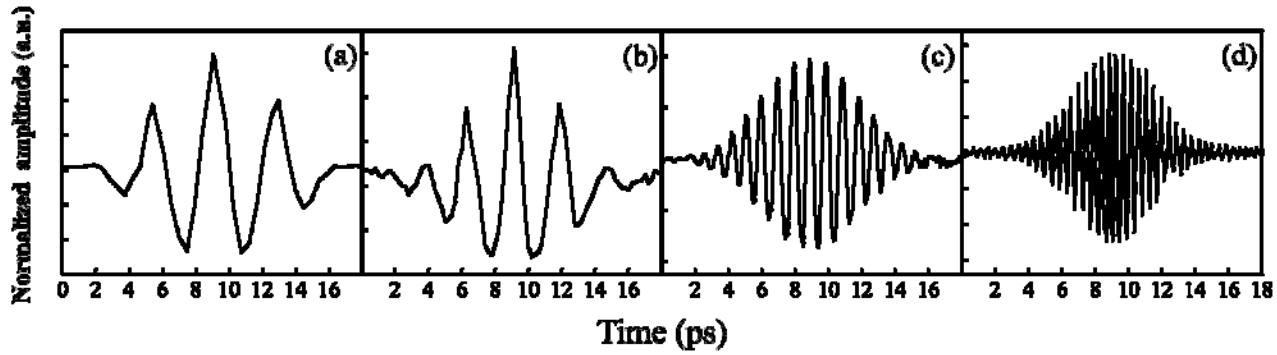

Figure 4. Measured field autocorrelation of THz radiation for time delay τ=0.4ps (a), 0.7ps (b), 1.8ps (c), and 3.6ps (d).

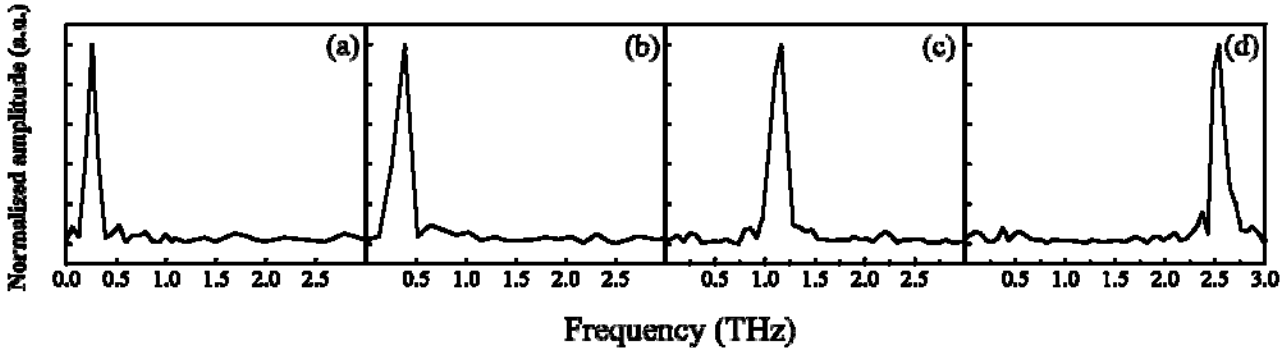

Figure 5. The spectra of THz radiation for time delay τ=0.4ps (a), 0.7ps (b), 1.8ps (c), and 3.6ps (d).

The variation of THz frequency is linearly dependent on the time delay τ, as shown in Figure 6. The THz energy is measured at different frequencies using a calibrated silicon bolometer (IR-Labs), which has a reasonably flat response across the spectrum of interest, and is shown in Figure 7. The THz pulse energy decreases with increasing radiation frequency. By focusing the radiation down to a ~2mm spot size , the THz electric field strength is estimated to be ~3×10^5 □ 10^6 V/m within the tunable frequency range of ~0.26-2.6THz.

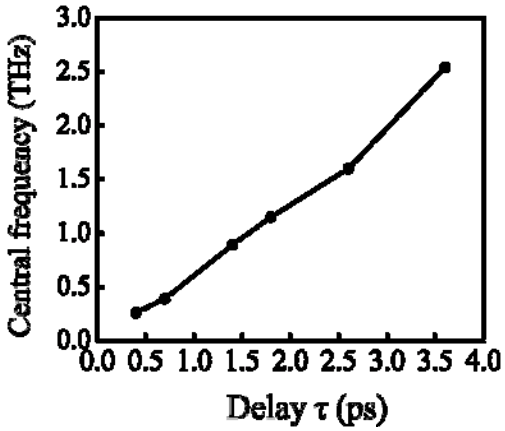

Figure 6. Variation of THz frequency as a function of time delay τ

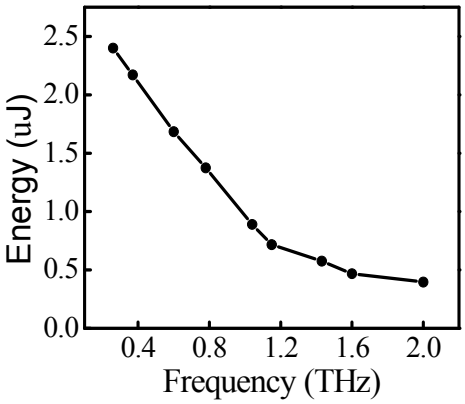

Figure 7. THz pulse energy as a function of radiation frequency

In summary, we have demonstrated the generation and characterization of tunable few-cycle and multi-cycle coherent THz pulses from ultrashort relativistic electron beams. We temporally shaped the photocathode drive laser using a chirped-pulse beating technique to produce quasi-sinusoidal intensity modulation at a tunable THz frequency, which in turn modulated the longitudinal density distribution of the electron bunches. By varying the time delay between the two chirped pulses, the modulation period of the electron bunches can be controlled. With less than ~100pC in an electron bunch, the temporal structure can be maintained through the acceleration, and few-cycle or multi-cycle THz pulses can be produced while the frequency of the THz radiation can be tuned from ~0.26 to 2.6 THz with the bandwidth of ~0.16 THz. The

frequency tunability is eventually limited by the space-charge effect. Our results have extended the capabilities of existing accelerator facilities as useful sources of THz radiation. Our study also indicates that it is possible to tailor the THz pulses and synthesize the THz waveform by the temporal shaping of the relativistic electron beam, which will open up new opportunities for studying the coherent control of physical and chemical dynamics of advanced materials.[20]

This work is supported by U.S. Department of Energy under Contract No. DE-AC02-98CH10886. The authors would like to thank Anthony Caracappa, Michael Fulkerson, Michael Lehecka, and Kenneth Pedersen for technical support and Houjun Qian for helpful discussion.

References

1. Y. Shen, T. Watanabe, D. A. Arena, C. C. Kao, J. B. Murphy, T. Y. Tsang, X. J. Wang, and G. L. Carr, Phys. Rev. Lett. **99**, 043901 (2007).
2. J. van Tilborg, C. B. Schroeder, Cs. Tóth, C. G. R. Geddes, E. Esarey, and W. P. Leemans, Opt. Lett. **32**, 313 (2007).
3. Y. Shen, G. L. Carr, J. B. Murphy, T. Y. Tsang, X. J. Wang, and X. Yang, Phys. Rev. A **78**, 043813 (2008).
4. A. S. Weling, B. B. Hu, N. M. Froberg, and D. H. Auston, Appl. Phys. Lett. **64**, 137, (1994).
5. J. Y. Sohn, Y. H. Ahn, D. J. Park, E. Oh, and D. S. Kima, Appl. Phys. Lett. **81**, 13 (2002).
6. Y. S. Lee,T. Meade, and T. B. Norris, Appl. Phys. Lett. **78**, 3583 (2002).
7. J. R. Danielson, A. D. Jameson, J. L. Tomaino, H. Hui, J. D. Wetzel, Y. S. Lee, and K. L. Vodopyanov, J. Appl. Phys. **104**, 033111, (2008).
8. J. M. Byrd, Z. Hao, M. C. Martin, D. S. Robin, F. Sannibale, R.W. Schoenlein, A. A. Zholents, and M. S.Zolotorev, Phys. Rev. Lett. **96,** 164801 (2006).

9. S. Bielawski, C. Evain, T. Hara, M. Hosaka, M. Katoh, S. Kimura, A. Mochihashi, M. Shimada, C. Szwaj, T. Takahashi, and Y. Takashima., Nature Phys. **4**, 390 (2008).
10. M. Boscolo, M. Ferrario, I. Boscolo, F. Castelli, and S. Cialdi, Nucl. Instr. and Meth. A **577** (2007) 409.
11. Y. Li, and K. Kim, Appl. Phys. Lett. **94**, 014101 (2008).
12. J. G. Neumann, R. B. Fiorito, P. G. O'Shea, H. Loos, B. Sheehy, Y. Shen, and Z. Wu, J. Appl. Phys. **105**, 053304 (2009).
13. Y.-E Sun, P. Piot, A. Johnson, A. H. Lumpkin, T. J. Maxwell, J. Ruan, and R. Thurman-Keup, Phys. Rev. Lett. **105**, 234801 (2010).
14. S. Liu, and Y. C. Huang, Nucl. Instr. and Meth. A **637** (2011) S172.
15. J. B. Murphy and X. J. Wang, Synchrotron Radiation News, **21**, 41 (2008).
16. X. J. Wang, X. Qiu, and I. Ben-Zvi, Phys. Rev. E **54**, R3121 (1996).
17. P. Piot, G. L. Carr, W. S. Graves, and H. Loos, Phys. Rev. ST Accel. Beams **6**, 033503 (2003).
18. D. X. Wang, G. A. Kraft, E. Price, P. A. D. Wood, D. W. Porterfield, and T. W. Crowe, Appl. Phys. Lett. **70**, 529 (1997).
19. C. J. Hirschmugl, M. Sagurton, and G. P. Williams, Phys. Rev. A **44**, 1316 (1991).
20. M. Mochizuki and N. Nagaosa, Phys. Rev. Lett. **105**, 147202 (2010).